Magnetotransport of $CeRhIn_5$

A. D. Christianson and A. H. Lacerda
National High Magnetic Field Laboratory, Los Alamos National Laboratory, Los Alamos, New Mexico 87545

M. F. Hundley, P. G. Pagliuso, and J. L. Sarrao
Condensed Matter and Thermal Physics Group, Los Alamos National Laboratory, Los Alamos, New Mexico 87545

(Received 10 September 2001; revised manuscript received 23 February 2002; published 9 August 2002)

We report measurements of the temperature-dependent anisotropic resistivity and in-plane magnetoresistance on single crystals of the tetragonal heavy-fermion antiferromagnet ($T_N = 3.8$ K) $CeRhIn_5$. The measurements are reported in the temperature range 1.4–300 K and in magnetic fields to 18 T. The resistivity is moderately anisotropic, with a room-temperature *c*-axis to in-plane resistivity ratio $\rho_c/\rho_a(300\ \mathrm{K}) = 1.7$. $\rho(T)$ measurements on the nonmagnetic analog $LaRhIn_5$ indicate that the anisotropy in the $CeRhIn_5$ resistivity stems predominantly from anisotropy in Kondo-derived magnetic scattering. In the magnetically ordered regime, an applied field H reduces T_N only slightly due to the small ordered moment ($0.37\mu_B$) and magnetic anisotropy. The magnetoresistance (MR) below T_N is positive and shows little sign of saturating in fields to 18 T. In the paramagnetic state, a positive MR is present below 7.5 K, while a high-field negative contribution is evident at higher temperatures. The positive contribution decreases in magnitude with increasing temperature. Above 40 K the positive contribution is no longer observable, and the MR is negative. The low-T positive MR results from interactions with the Kondo-coherent state, while the high-T negative MR stems from single-impurity effects. In general, these results indicate that $CeRhIn_5$ exhibits a modest degree of transport anisotropy not atypical among heavy-fermion compounds.

DOI: 10.1103/PhysRevB.66.054410 PACS number(s): 74.70.Tx, 71.27.+a, 75.40.Cx

I. INTRODUCTION

Transport measurements in large applied magnetic fields provide an exceptionally useful means of probing the electronic and thermodynamic properties of heavy-fermion compounds. This stems from the magnetic origin of the interactions responsible for the mass-enhanced ground state.[1] As such, the resistivity of a heavy-fermion system is altered by an applied magnetic field in fundamentally different ways when the compound is in a magnetically ordered, Kondo-coherent or single-impurity regime. Field-dependent measurements can also provide information regarding the importance of magnetic fluctuations and the proximity to low-temperature magnetic instabilities in the coherent regime. Although no complete microscopic theory is available to fully model the transport and thermodynamic properties of a heavy-fermion system, a number of theoretical treatments are available that qualitatively describe the key features of a system's field-dependent behavior.[2,3] From the experimental point of view, a wide range of phenomena can be observed when applying a magnetic field at low temperature.[4] Among archetype heavy-fermion compounds, UPt_3 and $CeRu_2Si_2$ exhibit highly anisotropic magnetotransport behavior and remarkable field-induced metamagnetic transitions at 20 T (Refs. 5 and 6) and 8 T (Ref. 7), respectively, while UBe_{13} exhibits negative magnetoresistance above its superconducting transition temperature.[8] Ultimately, a heavy-fermion system's field-dependent properties are determined by Ruderman-Kittel-Kasuya-Yosida (RKKY) and Kondo interactions,[9] with the relative importance of these two interactions influenced by magnetic and structural anisotropies.

A new family of Ce-based heavy fermions was recently discovered that exhibits a complex phase diagram that challenges our understanding of correlated-electron physics.[10,11] This family has a generalized chemical formula, $Ce_mM_nIn_{3m+2n}$, where M is Rh, Ir, or Co. All compounds investigated to date ($m = 1,2$ and $n = 1$), except cubic $CeIn_3$, crystallize in a tetragonal structure (space group $P4/mmm$).[12] The most notable properties in this series of compounds include ambient-pressure magnetic order ($T_N = 3.8$ K) and pressure-induced superconductivity ($T_c = 2.1$ K at 16 kbar pressure) in $CeRhIn_5$,[10,13,14] and unconventional[15] ambient-pressure superconductivity in both $CeIrIn_5$ [$T_c = 0.4$ K (Ref. 16)] and $CeCoIn_5$ [$T_c = 2.3$ K (Ref. 17)]; the transition temperature for $CeCoIn_5$ is the highest ambient-pressure T_c reported to date for a heavy-fermion superconductor. This new family of compounds offers the opportunity to explore the importance of tuned dimensionality and/or anisotropy on magnetic, Kondo, and superconducting groundstates.

$CeRhIn_5$ has attracted considerable attention due to its unusual pressure-temperature phase diagram.[10] Ce heavy-fermion systems that order antiferromagnetically typically exhibit a P-T phase diagram wherein applied pressure acts to smoothly reduce the Néel temperature T_N to zero at a critical pressure P_c, with superconductivity occurring over a range of pressure centered at P_c. The P-T phase diagram of the cubic member of the $Ce_mM_nIn_{3m+2n}$ family ($CeIn_3$) displays this behavior, with an ambient-pressure ordering temperature $T_N = 10$ K, a slightly enhanced Sommerfeld coefficient of 100 mJ/mol K^2, and a critical pressure $P_c = 23$ kbar.[18,19] The $CeRhIn_5$ P-T phase diagram is quite different. At ambient pressure, $CeRhIn_5$ orders antiferromagnetically at 3.8 K. Applied hydrostatic pressure acts to very slightly increase T_N until magnetic order becomes unobservable near 16 kbar, at which point superconductivity appears

at 2.1 K.[10] Specific-heat measurements indicate an enhanced Sommerfeld coefficient of roughly 420 mJ/mol K^2 below 10 K;[10] for a single-impurity system,[20] this corresponds to a Kondo temperature of roughly 10 K. $CeRhIn_5$ has a quasi-two-dimensional structure that is composed of alternating layers of the cubic heavy-fermion antiferromagnet $CeIn_3$ and a transition-metal layer composed of $RhIn_2$. As such, dimensionality may play a role in the interactions that produce the unusual *P-T* phase diagram exhibited by $CeRhIn_5$. This is borne out by nuclear quadrupolar resonance[21] and neutron scatting measurements[22] that indicate that the magnetic moments lie in the basal plane of the tetragonal structure with a spiral along the *c* axis, with a reduced magnetic moment of 0.37 Bohr magneton (μ_B). However, recent inelastic neutron scattering experiments indicate some degree of three-dimensional behavior for $CeRhIn_5$.[23] Clearly, further measurements are needed to fully elucidate the influence of dimensionality on the physical properties of $CeRhIn_5$.

In order to enhance our understanding of the ground-state properties of $CeRhIn_5$, we have measured the anisotropic resistivity of this compound as a function of magnetic field and temperature. The resistivity is moderately anisotropic, with a room-temperature *c*-axis to in-plane resistivity ratio ρ_c/ρ_a of 1.7. This ratio changes markedly with decreasing temperature, and at 4 K the in-plane resistivity is larger than the out-of-plane resistivity by 80%. The antiferromagnetic transition at 3.8 K produces an inflection point in ρ. With application of magnetic field, the transition moves to slightly lower temperatures, with a field dependence that depends upon the direction of the applied field. The magnetoresistance (MR) also depends upon the direction of the applied field, and it appears to be only moderately influenced by structural anisotropy. The MR is positive in the magnetically ordered state and shows little sign of saturating, except possibly at the lowest temperature for $H\|c$. At moderate temperatures, we observe a positive contribution to the MR that is characteristic of a Kondo system in the coherent regime. At higher temperature, this positive MR gives way to a negative contribution characteristic of a single-impurity Kondo system.

II. EXPERIMENTAL DETAILS

Single crystals of $CeRhIn_5$ were grown from an In flux method[24] as described previously.[12] The deleterious influence of residual In flux on low-*T* transport measurements (the superconducting transition for In occurs at 3.4 K) necessitates careful sample surface polishing to remove any possible In contamination. The polished single-crystal samples were oriented using Laue x-ray diffraction to determine the crystallographic in-plane (*a*-axis) and out-of-plane (*c*-axis) directions. Finally, the resistance of each sample that was slated for use in MR measurements was measured down to 2 K to ensure that no extrinsic superconductivity contamination was evident at 3.4 K due to surface In. The samples that passed this screening process had residual resistivity ratios [RRR $=\rho(300\ \mathrm{K})/\rho(2\ \mathrm{K})\approx 100$] that were similar to those reported previously.[25]

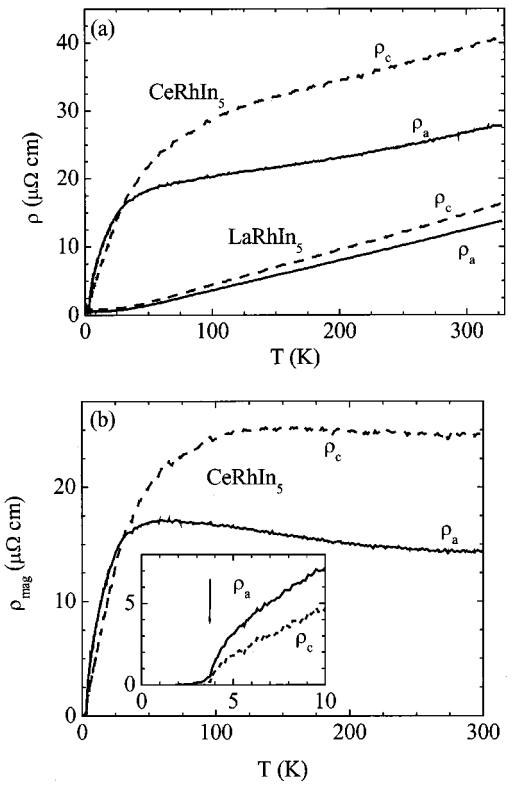

FIG. 1. (a) In-plane (solid lines) and *c*-axis (dashed lines) temperature-dependent resistivities of $CeRhIn_5$ and the nonmagnetic analog $LaRhIn_5$. (b) The in-plane (solid line) and *c*-axis (dashed line) magnetic resistivity ($\rho_{mag}=\rho_{Ce}-\rho_{La}$) of $CeRhIn_5$. The data near T_N are highlighted in the inset, with the arrow positioned at T_N.

All resistivity measurements reported here were made with a conventional four-probe sample configuration in which silver conductive paint or epoxy was used to make sample contacts. Sample resistances were measured with a low-frequency ac bridge. The in-plane and out-of-plane resistivities were determined on oriented samples via the Montgomery and anisotropic van der Pauw methods.[26] The transverse magnetoresistance was measured with current applied along an *a* axis, and the applied field oriented perpendicular to the measurement current (i.e., either in the other *a* axis or along the *c* axis). The transport measurements were carried out in a variable-flow cryostat capable of temperatures from 1.4 to 325 K. To avoid magnetoresistance effects in the Cernox thermometer used to determine and control sample temperature, temperatures below 3 K were stabilized by controlling the ^{4}He vapor pressure.

III. RESULTS

The temperature-dependent resistivities of $CeRhIn_5$ and $LaRhIn_5$ in, and perpendicular to, the basal plane, are shown in Fig. 1(a). The data for $CeRhIn_5$ indicate that this compound is moderately anisotropic; ρ_c is roughly 70% larger

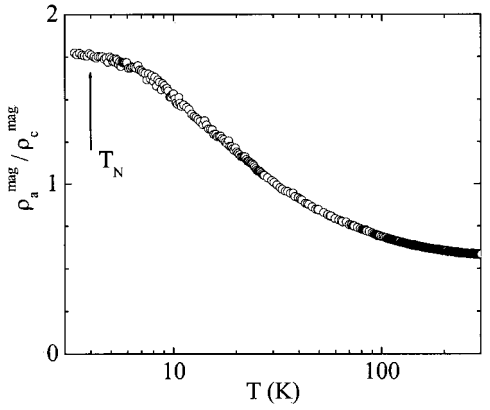

FIG. 2. Temperature-dependent magnetic resistivity anisotropy ratio ($\rho_a^{mag}/\rho_c^{mag}$) of $CeRhIn_5$.

than ρ_a at room temperature. Below 325 K the resistivity falls with decreasing temperature in both directions, and both ρ_a and ρ_c exhibit shoulderlike features between 50 and 100 K. Both resistivities fall off more rapidly at lower temperatures. ρ_a and ρ_c cross at 30 K, and the *a*-axis resistivity is larger than the *c*-axis resistivity down to 1 K. In comparison, the resistivity of $LaRhIn_5$ (the nonmagnetic analog of $CeRhIn_5$) varies linearly with temperature below 300 K, and saturates to a value near 1 $\mu\Omega$ cm below 20 K. The $LaRhIn_5$ *c*-axis resistivity is greater than the in-plane resistivity at all temperatures, and the anisotropy ratio ρ_c/ρ_a is nearly *T*-independent. The 300-K anisotropy ratio $\rho_c/\rho_a=1.2$ for $LaRhIn_5$ suggests that the nonmagnetic electronic anisotropy inherent to the $RMIn_5$ structure is relatively small.

The temperature-dependent magnetic scattering component ($\rho_{mag}=\rho_{Ce}-\rho_{La}$) of the $CeRhIn_5$ in-plane and *c*-axis resistivities are presented in Fig. 1(b). After removing the electron-phonon scattering contribution to ρ_{Ce}, the magnetic resistivity in both crystallographic directions varies as $\rho\propto -\ln(T)$ at high temperatures and drops sharply below 50 K; this *T* dependence is characteristic of Kondo lattice compounds.[1] The resistivity in the vicinity of the 3.8-K antiferromagnetic (AFM) transition is shown in the inset to Fig. 1(b). A clear change in magnetic scattering is evident in both ρ_a and ρ_c near T_N. The transport anisotropy ratio $\rho_a^{mag}/\rho_c^{mag}$ is plotted as a function of temperature in Fig. 2. Near room temperature the magnetic resistivity is moderately anisotropic ($\rho_a^{mag}/\rho_c^{mag}$ at 300 K is 0.6), and the ratio exhibits a gradual evolution from a high-*T* regime where $\rho_a^{mag}/\rho_c^{mag}<1$ to a low-*T* regime where $\rho_a^{mag}/\rho_c^{mag}>1$. The magnetic resistivities cross at 30 K. ρ_c^{mag} is smaller than ρ_a^{mag} down to the lowest measurement temperature (1.4 K), and there is no evidence for any change in $\rho_a^{mag}/\rho_c^{mag}$ at or below T_N.

We now turn to an examination of the influence of applied magnetic fields on the *T*-dependent in-plane resistivity. The resistivity as a function of temperature in a field of 18 T is displayed in Fig. 3, and compared to the zero-field ρ_a data. In Fig. 3(a) the magnetic field is applied parallel to the basal plane and perpendicular to the current. A positive MR is evident at low temperatures, with the magnitude of the effect diminishing with increasing temperature. Above roughly 50

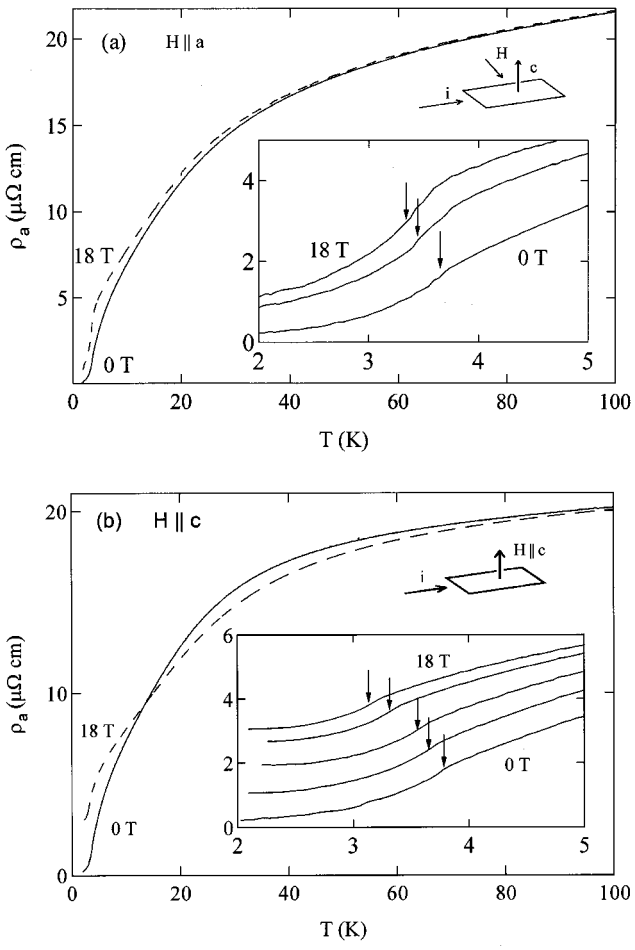

FIG. 3. In-plane temperature-dependent resistivity in an applied magnetic field. In (a) the magnetic field is applied in the basal plane (perpendicular to the current). The inset displays an expanded view near the AFM transition (the curves correspond to $\mu_0H=0$, 10, and 18 T). The arrows mark the inflection point in ρ (located at 3.70, 3.45, and 3.35 K). In (b) the field is applied along the *c* axis. The curves in the inset correspond to $\mu_0H=0$, 5, 10, 15, and 18 T, where the inflection points are located at 3.80, 3.70, 3.60, 3.30, and 3.10 K, respectively. For both field directions a small amount of scatter in the $\rho(T)$ data leads to an uncertainty in determining T_N of ± 50 mK.

K, no difference is discernable between $\rho(H=0)$ and ρ(18 T). The inset to Fig. 3(a) shows $\rho(T)$ in fields of 0, 10, and 18 T in the vicinity of T_N; in this temperature regime the applied fields appear to uniformly increase the resistivity below 4 K. The *H*-dependent AFM ordering temperature can be determined by finding the location of the inflection point in ρ that marks T_N.[27] The arrows in the inset denote $T_N(H)$. The transition moves downward monotonically with temperature; in 18 T the inflection point occurs at 3.35 K, corresponding to the rate $dT_N/dH_{\|}=-25$ mK/T. The *a*-axis resistivity for a field applied parallel to the *c* axis is shown in Fig. 3(b). In this field orientation, the low-*T* magnetoresistance is also positive, but the 18-T MR crosses zero at 16 K and becomes large and negative at higher temperatures. This negative MR effect reaches a maximum value nearly 30 K. At higher temperatures the negative MR diminishes in magnitude, ap-

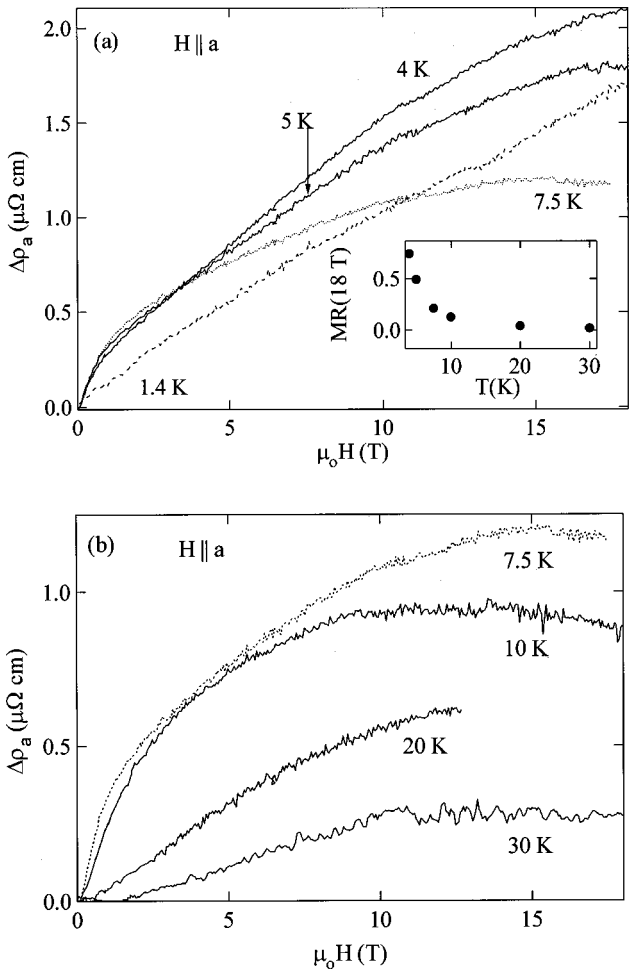

FIG. 4. In-plane field-induced change in resistivity $\Delta\rho=\rho(H)-\rho(0)$ $(H\|a)$. The low-T behavior is featured in (a). The inset shows the magnetoresistance $\Delta\rho/\rho(0)$ at 18 T for $T<30$ K. The value for the 1.4-K magnetoresistance at 18 T $[\Delta\rho/\rho(0)=8.7]$ is not displayed due to its large magnitude. The high-temperature behavior of $\Delta\rho$ is displayed in (b).

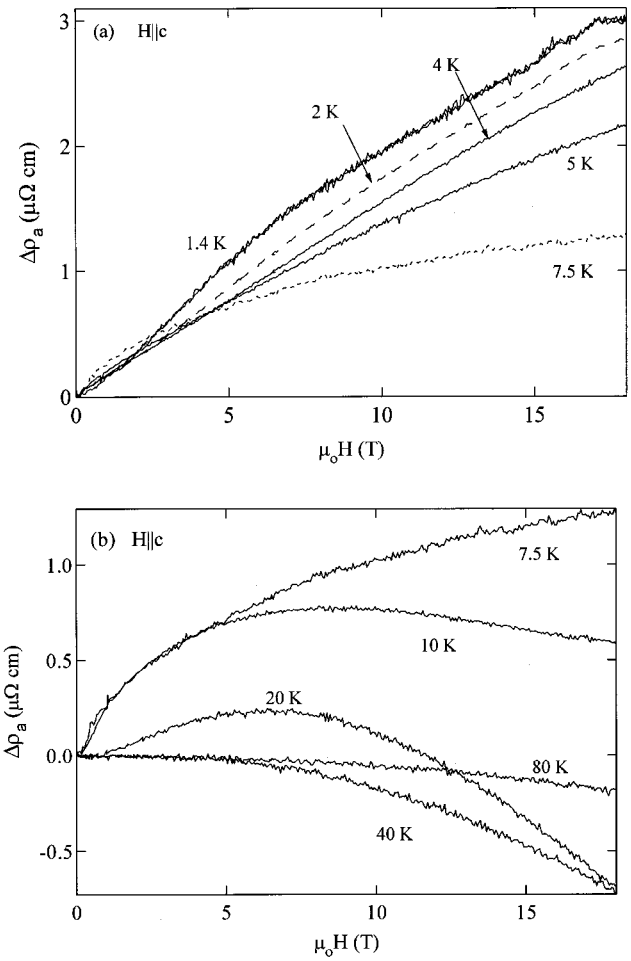

FIG. 5. In-plane field-induced change in resistivity $\Delta\rho=\rho(H)-\rho(0)$ $(H\|c)$. The low-T behavior is featured in (a). The high-temperature behavior of $\Delta\rho$ is displayed in (b).

proaching zero at 100 K. The inset to Fig. 3(b) depicts $\rho(T)$ in fields of 0, 5, 10, 15, and 18 T in the vicinity of T_N; as with the in-plane field orientation, the applied field uniformly increases ρ_a below 5 K. The field also decreases the AFM transition temperature, but at a faster rate than for fields oriented in the basal plane. In 18 T the applied field drops T_N to 3.0 K; this corresponds to a rate $dT_N/dH_\perp=-35$ mK/T, a value that is in good agreement with previous $C_p(H,T)$ measurements.[28,33]

The field-dependent in-plane magnetoresistance $\Delta\rho_a(H)=\rho_a(H)-\rho_a(H=0)$ at constant temperature is depicted in Figs. 4 $(H\|a)$ and 5 $(H\|c)$ for $CeRhIn_5$. With the field applied in the basal plane the MR below 10 K [Fig. 4(a)] exhibits two distinct regimes. At 1.4 K the $\Delta\rho_a(H)$ varies linearly with H throughout the measured field range $(H\leqslant 18$ T), while for $T>T_N$ the MR grows in magnitude and exhibits some curvature below 5 T. At 7.5 K the MR varies as $H^{1/2}$ above 1 T, and it saturates above 15 T. At still higher temperatures [Fig. 4(b)] $\Delta\rho_a(H)$ displays a broad maximum that occurs near $H_{\max}=12$ T. The rise in the MR at low fields is suppressed as the temperature is increased, and the overall magnitude of the magnetoresistance diminishes as well. The relative magnetoresistance in 18 T, defined as $[\rho_a(H)-\rho_a(H=0)]/\rho_a(H=0)$, is plotted as a function of temperature in the inset to Fig. 4(a). The relative MR is nearly zero above 20 K and grows markedly below 10 K in large measure due to the sharp drop in $\rho_a(T,H=0)$ that stems from the onset of coherence. In contrast, the magnetoresistance of the nonmagnetic analog $LaRhIn_5$ displays a standard metallike positive MR that varies as H^2 and diminishes in magnitude with increasing temperature.

The in-plane magnetoresistance of $CeRhIn_5$ with H applied along the c axis is depicted in Fig. 5. For $T\leqslant 7.5$ K [Fig. 5(a)] the results are qualitatively similar to those for $H\|a$. Below T_N $\Delta\rho_a(H)$ is positive, with a small change in slope evident near 2.5 T. There is little sign of saturation, except possibly the appearance of a feature of unknown origin at ~17 T and 1.4 K. Above T_N the high-field MR grows as H^α with $\alpha<1$. At 7.5 K $\Delta\rho_a(H)$ varies as $H^{1/2}$ throughout the measured field range, and it is approaching saturation at 18 T. For $T\geqslant 7.5$ K [Fig. 5(b)] the MR is quite different from

the low-T behavior. The $H^{1/2}$ behavior present at 7.5 K evolves into a peak in $\Delta\rho_a(H)$ at 10 K that occurs between 5 and 10 T, and the MR decreases markedly at still higher fields. Above 20 K, the low-H positive MR is no longer in evidence and the negative MR contribution predominates. The MR is negative above 30 K at all fields, and the overall magnitude of the negative MR decreases with increasing temperature.

Taken as a whole, the temperature and magnetic-field-dependent ρ_a data presented in Figs. 3–5 suggest that there are three field-dependent transport regimes in $CeRhIn_5$. The first, in the magnetically ordered state, exhibits a large positive MR that shows little sign of saturation at 18 T (we note that at least 40 T is required to field-polarize the AFM state).[29] The second regime resides in the paramagnetic state just above T_N. In this regime the MR is positive and exhibits a tendency to saturate near 20 T. The third regime occurs at temperatures above 10 K and at high fields where a negative MR contribution comes into play that initially produces a maximum in $\Delta\rho_a(H)$. At still higher temperatures, the positive MR disappears and the negative contribution dominates the field-dependent transport. Magnetic anisotropy influences the detailed nature of the field-dependent transport. The influence of the high-T negative MR contribution is largest with the field applied perpendicular to the basal plane. As such, the peak field $H_{\max}$ is largest with the field applied in the basal plane, and the MR is more negative for $H\|c$.

IV. DISCUSSION

The anisotropy in the zero-field resistivity data and the complex H field and T dependence of the a-axis magnetoresistance are the most prominent features of these $CeRhIn_5$ magnetotransport data. How do these features reflect the tetragonal crystal structure, the Kondo and crystal-field interactions, and the RKKY-mediated antiferromagnetic order? Before answering these questions, we first must examine the influence that lattice anisotropy has on the electronic and magnetic structure in the $CeRhIn_5$.

The $CeRhIn_5$ unit cell is composed of cubic $CeIn_3$ building blocks that are separated by $RhIn_2$ layers. Full-potential band-structure calculations[30] indicate that the electronic structure of $CeRhIn_5$ and $LaRhIn_5$ reflects the quasi-two-dimensional nature of the tetragonal unit cell. The band structure exhibits a number of bands that cross the Fermi energy E_F, producing three Fermi surfaces. Only the first, containing holelike orbits, is relatively isotropic. Reflecting $CeRhIn_5$'s planar structure, the second and third surfaces are composed of corrugated cylindrical electronlike and holelike orbits that extend along the c axis. de Haas–van Alphen (dHvA) measurements detect extremal orbits that are consistent with the band-structure calculations.[25,30] In addition, the Hall effect in both $CeRhIn_5$ and $LaRhIn_5$ is anisotropic and strongly temperature dependent,[31] providing clear evidence for competing electron and hole carriers. The fact that the Hall effect in $CeRhIn_5$ and $LaRhIn_5$ are quite similar indicates that they share the same anisotropic electronic structure, and that the f electrons in $CeRhIn_5$ are localized.[32] Hence, from both measurement and calculation, the layered structure of $CeRhIn_5$ is reflected in the compound's complex electronic structure.

The magnetic structure of the antiferromagnetic ground state also reflects $CeRhIn_5$'s layered nature. The magnetic moments that order at $T_N = 10$ K in $CeIn_3$ are commensurate with the cubic lattice.[19] In contrast, the magnetic moments in $CeRhIn_5$ are found to lie completely within the basal plane, and they form an incommensurate spiral along the c axis.[21,22] Field-dependent specific-heat[33] and dHvA[25] measurements indicate that fields oriented along the c axis gradually reduce the ordering temperature without altering this incommensurate structure. Fields applied within the basal plane strongly influence the magnetic structure, producing a complex H-T phase diagram.[29,33,34] Below 3 K a field of 2 T transforms the magnetic structure to one that is commensurate with the lattice, while a third state is also present near 3.5 K. The onset ordering temperature is much less field-dependent than that for $H\|c$. In the paramagnetic regime the magnetic susceptibility χ exhibits a factor-of-2 anisotropy between χ_a and χ_c.[10] This anisotropy stems from the splitting of the $J=\frac{5}{2}$ manifold under the influence of tetragonal crystalline electric fields. The crystal-field level scheme that describes $\chi_a(T)$ and $\chi_c(T)$ in the paramagnetic state[35] includes a Γ_7 doublet ground state (composed predominantly of the $|\pm\frac{5}{2}\rangle$ spin state), a first-excited Γ_7 doublet (predominantly $|\pm\frac{3}{2}\rangle$) at 6 meV, and the last state, a spin-$\frac{1}{2}$ Γ_6 doublet, located 13 meV above the Γ_7 ground state. This level scheme is generally consistent with recent inelastic neutron scattering results.[36] Armed with this information concerning $CeRhIn_5$'s electronic and magnetic structures, as well as the crystal-level scheme, we can now examine the underlying mechanisms responsible for the magnetotransport features exhibited by $CeRhIn_5$.

The modest transport anisotropy exhibited by $LaRhIn_5$ ($\rho_c/\rho_a \approx 1.2$) indicates that the quasi-2D electronic structure does not translate into transport anisotropy. Conventional electron-phonon scattering also appears to be weakly influenced by the planar 1:1:5 structure as well. The absence of significant anisotropy in the resistivity of $LaRhIn_5$ indicates that the anisotropy in the $CeRhIn_5$ resistivity stems from magnetic scattering. Both the a-axis and c-axis magnetic resistivities of $CeRhIn_5$ display temperature dependencies that are characteristic of a Kondo-lattice compound. The complex T-dependent anisotropy between the a- and c-axis magnetic resistivities is reminiscent of that seen in many other heavy-electron systems. For example, the a-axis and c-axis resistivities in the tetragonal compounds $CeRu_2Si_2$ and $CeNi_2Ge_2$ also cross in a manner reminiscent of $CeRhIn_5$.[37,38] There are also a number of other f-electron compounds that exhibit an anisotropic ρ_{mag} but without any crossing of the ρ_a and ρ_c resistivities. Systems that fall into this second class include the hexagonal compound UPt_3,[39] orthorhombic $CeCu_6$,[40] and the tetragonal compounds $CePt_2Si_2$,[41] $CePd_2Si_2$,[42] and $CeCu_2Si_2$.[43] As with $CeRhIn_5$, ρ_a and ρ_c never differ by more than a factor of 2 in these systems. These resistivity anisotropies can be explained by considering the nature of the scattering relaxation rates that are produced when resonant Kondo scattering is influenced by anisotropic

crystal-field levels.[44,45] This modeling describes successfully the anisotropy evidenced by a wide variety of Ce compounds.[41,44–46] As such, it seems reasonable to conclude that the magnetic resistivity anisotropy in $CeRhIn_5$ is a reflection of anisotropic carrier scattering due to the influence of the crystal fields.

The influence of an applied magnetic field on the resistivity near the antiferromagnetic transition is depicted in the insets to Figs. 3(a) and 3(b). The zero-field AFM order at $T_N = 3.8$ K gives rise to an inflection point in the resistivity, indicating that magnetic order alters the transport in at most a modest way. The absence of any abrupt change in the ratio ρ_a/ρ_c at T_N indicates that the onset of magnetic order influences spin-wave scattering isotropically; this is consistent with inelastic neutron scattering measurements[23] that indicate that there is no three-dimensional (3D) to 2D crossover prior the onset of long-range order and that the magnetic system is predominantly three-dimensional. Specific-heat[33] measurements show that a magnetic field applied in the basal plane will split the antiferromagnetic transition into three separate transitions. Preliminary neutron-diffraction measurements[34] indicate that these transitions are associated with an evolution in the zero-field magnetic structure. No such splitting of the antiferromagnetic transition signature is evident in the resistivity data shown in the Fig. 3(a) inset. This may be due to the relatively small change in carrier scattering that will occur when the system is transformed from one magnetic structure to the next; as such, the resistivity inflection points pertaining to the reorientation transitions may be unobservable. However, the inflection point [determined by finding the maximum of $d\rho(H,T)/dT$], as indicated by the arrows in the inset, decreases very gradually ($dT_N/dH_{\parallel} = -25$ mK/T) with magnetic field. Specific-heat measurements[28,33] with the magnetic field applied along the c axis indicate that while the field does not alter the magnetic structure it does have a stronger influence on T_N; this is consistent with the more rapid field-induced decrease in the inflection-point temperature ($dT_N/dH_{\perp} = -35$ mK/T) evident in the data displayed in the Fig. 3(b) inset. We note that the inflection point at zero applied field occurs at 3.7 ± 0.05 K in one case [Fig. 3(a) inset] and at 3.8 ± 0.05 K [Fig. 3(b) inset]. This difference is merely an indication of the error in determining the maximum in $d\rho/dT$. Despite this moderate error, the trend of T_N to lower temperature with increasing applied field emerges and is in agreement with previous thermodynamic measurements.[28,33]

We now consider the magnetoresistance in the paramagnetic state. The data exhibit two field-temperature regimes: at low H and T the MR is positive, while at high H and T the MR exhibits a negative contribution. A similar low-T positive MR has been reported in both $CeAl_3$ (Refs. 47 and 48) and $CeRu_2Si_2$ (Ref. 49) at low temperatures and in UBe_{13} under pressure.[50] The similarity between $CeRhIn_5$ and these other compounds suggests that a low-temperature positive MR appears to be a common feature of Kondo systems that are in, or are approaching, a coherent Fermi-liquid state.[3,51] Despite many attempts,[2,3,52] no satisfactory detailed theoretical explanation for the positive MR in the low-T paramagnetic state has been put forward. For now we can only say

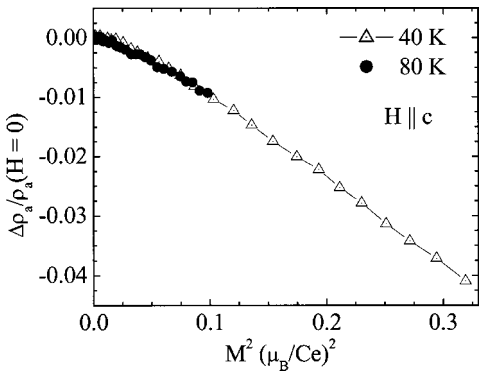

FIG. 6. In-plane magnetoresistance $\Delta\rho_a/\rho_0$ at 40 and 80 K plotted as a function of the magnetization squared. H is applied along c, and the M^2 units are Bohr magnetons per Ce atom.

that this effect must reflect the influence of an applied H field on the Kondo-coherent state. In the single-impurity regime our understanding of MR effects rests on firmer ground. In this regime an applied field reduces incoherent Kondo scattering, producing a negative MR.[53,54] In this situation the MR is known to scale with the induced magnetization M as $\Delta\rho/\rho_0 \propto -M^2$.[54] Hence, a plot of $\Delta\rho/\rho_0(M)$ for all H and T should fall onto a single, universal curve. A careful analysis of the magnetoresistance data for all temperatures that exhibit a hint of a negative MR is made problematic by the interaction between the low-H positive effect and the high-H negative contribution. Nonetheless, this single-impurity analysis is possible with $H \| c$ for $T \geqslant 40$ K, as the MR shows no positive contribution in this temperature range. These data are plotted as a function of M^2 in Fig. 6. The data scale as expected, falling on a common line and varying as M^2. Hence, the negative high-temperature MR contribution appears to be a simple-impurity effect. At these temperatures the applied field reduces incoherent Kondo scattering, giving rise to a negative MR. The detailed nature of the MR and in particular the stronger negative contribution for $H \| c$ are an indication that the magnetic anisotropy evident in ρ_{mag} also influences the detailed balance between coherent and incoherent MR effects in $CeRhIn_5$. As such, the temperature-dependent $CeRhIn_5$ magnetotransport reflects the prevalent Kondo regime (coherent at low T, single impurity at high T) as well as the magnetic anisotropy stemming from the nature of the crystal-field levels.

V. CONCLUSIONS

Structural anisotropy influences the physical properties of $CeRhIn_5$ in a subtle but significant way. Tetragonal crystalline electric fields split the $J = \frac{5}{2}$ manifold into three doublets whose anisotropy influences both the magnetic susceptibility[10] and the zero-field resistivity. The $RhIn_2$ spacer layer alters the c-axis magnetic exchange sufficiently to produce antiferromagnetism with an incommensurate spiral spin structure.[21,22] Dimensionality effects are also evident in the way an applied H field alters this spin arrangement.[33,34] Both dHvA[25,30] and Hall-effect[31] measure-

ments indicate that $CeRhIn_5$'s electronic structure has two-dimensional character. And, finally, while the overall field- and temperature-dependent MR in the paramagnetic regime is predominately determined by Kondo-lattice and single-impurity Kondo interactions, the detailed interplay between these positive and negative MR contributions manifests the impact of anisotropy on the magnetotransport. Magnetotransport measurements are underway on the ambient-pressure superconducting members of the 1:1:5 family ($CeIrIn_5$ and $CeCoIn_5$) to determine the relative importance of structural and magnetic (crystalline electric field) anisotropy in these systems as well.

ACKNOWLEDGMENTS

We gladly acknowledge useful discussions with J. M. Lawrence (University of California, Irvine) and S. Kern (Colorado State University). The work at Los Alamos National Laboratory was performed under the auspices of the U.S. Department of Energy. The work at the National High Magnetic Field Laboratory, Los Alamos Facility was performed under the auspices of the National Science Foundation, the State of Florida, and the U.S. Department of Energy. One of us (A.D.C.) would like to acknowledge partial support from the Manuel Lujan Jr. Neutron Scattering Center (Los Alamos National Laboratory).

[1] For a review, see Z. Fisk, D. W. Hess, C. J. Pethick, D. Pines, J. L. Smith, J. D. Thompson, and J. O. Willis, Science **239**, 33 (1988); Z. Fisk, J. L. Sarrao, J. L. Smith, and J. D. Thompson, Proc. Natl. Acad. Sci. U.S.A. **92**, 6663 (1995).

[2] F. J. Ohkawa, Phys. Rev. Lett. **64**, 2300 (1990).

[3] A. Lorek, N. Grewe, and F. B. Anders, Solid State Commun. **78**, 167 (1991).

[4] J. J. M. Franse, Physica B **155**, 236 (1989).

[5] P. H. Frings, J. J. M. Franse, F. R. de Boer, and A. Menovsky, J. Magn. Magn. Mater. **31–34**, 240 (1983).

[6] A. de Visser, R. Gersdorf, J. J. M. Franse, and A. Menovsky, J. Magn. Magn. Mater. **54–57**, 383 (1986).

[7] P. Haen, J. Flouquet, F. Lapierre, P. Lejay, and G. Remenyi, J. Low Temp. Phys. **67**, 391 (1987).

[8] U. Rauchschwalbe, F. Steglich, and H. Rietschel, Europhys. Lett. **1**, 71 (1986).

[9] S. Doniach, in *Valence Instabilities and Related Narrow Band Phenomena*, edited by R. D. Parks (Plenum, New York, 1977), p. 169.

[10] H. Hegger, C. Petrovic, E. G. Moshopoulou, M. F. Hundley, J. L. Sarrao, Z. Fisk, and J. D. Thompson, Phys. Rev. Lett. **84**, 4986 (2000).

[11] J. D. Thompson, R. Movshovich, Z. Fisk, F. Bouguet, N. J. Curro, R. A. Fisher, P. C. Hammel, H. Hegger, M. F. Hundley, M. Jaime, P. G. Pagliuso, C. Petrovic, N. E. Phillips, and J. L. Sarrao, J. Magn. Magn. Mater. **226**, 5 (2001).

[12] E. G. Moshopoulou, Z. Fisk, J. L. Sarrao, and J. D. Thompson, J. Solid State Chem. **158**, 25 (2001), and references therein.

[13] Y. Kohori, Y. Yamato, Y. Iwamoto, and T. Kohara, Eur. Phys. J. B **18**, 601 (2000); T. Mito, S. Kawasaki, G. Q. Zheng, Y. Kawasaki, K. Ishida, Y. Kitaoka, D. Aoki, Y. Haga, and Y. Onuki, Phys. Rev. B **63**, 220507(R) (2001).

[14] R. A. Fisher, F. Bouquet, N. E. Phillips, M. F. Hundley, P. G. Pagliuso, J. L. Sarrao, Z. Fisk, and J. D. Thompson (unpublished).

[15] R. Movshovich, M. Jaime, J. D. Thompson, C. Petrovic, Z. Fisk, P. G. Pagliuso, and J. L. Sarrao, Phys. Rev. Lett. **86**, 5152 (2001).

[16] C. Petrovic, R. Movshovich, M. Jaime, P. G. Pagliuso, M. F. Hundley, J. L. Sarrao, Z. Fisk, and J. D. Thompson, Europhys. Lett. **53**, 354 (2001).

[17] C. Petrovic, P. G. Pagliuso, M. F. Hundley, R. Movshovich, J. L. Sarrao, J. D. Thompson, and Z. Fisk, J. Phys.: Condens. Matter **13**, L337 (2001).

[18] I. R. Walker, F. M. Grosche, D. M. Freye, and G. G. Lonzarich, Physica C **282–287**, 303 (1997).

[19] N. D. Mathur, F. M. Grosche, S. R. Julian, I. R. Walker, D. M. Freye, R. K. W. Haselwimmer, and G. G. Lonzarich, Nature (London) **394**, 39 (1998).

[20] V. T. Rajan, Phys. Rev. Lett. **51**, 308 (1983).

[21] N. J. Curro, P. C. Hammel, P. G. Pagliuso, J. L. Sarrao, J. D. Thompson, and Z. Fisk, Phys. Rev. B **62**, 6100 (2000).

[22] Wei Bao, P. G. Pagliuso, J. L. Sarrao, J. D. Thompson, Z. Fisk, J. W. Lynn, and R. W. Erwin, Phys. Rev. B **62**, 14 621 (2000); **63**, 219901(E) (2001).

[23] Wei Bao, G. Aeppli, J. W. Lynn, P. G. Pagliuso, J. L. Sarrao, M. F. Hundley, J. D. Thompson, and Z. Fisk, Phys. Rev B **65**, 100505 (2002).

[24] P. C. Canfield and Z. Fisk, Philos. Mag. B **65**, 1117 (1992).

[25] A. L. Cornelius, A. J. Arko, J. L. Sarrao, M. F. Hundley, and Z. Fisk, Phys. Rev. B **62**, 14 181 (2000).

[26] H. C. Montgomery, J. Appl. Phys. **42**, 2971 (1971); B. F. Logan, S. O. Rice, and R. F. Wick, *ibid.* **42**, 2975 (1971); L. J. Van der Pauw, Philips Res. Rep. **13**, 1 (1958); W. L. V. Price, Solid-State Electron. **16**, 753 (1973).

[27] Scatter in the $\rho(T)$ data below 4 K leads to some uncertainty in determining the location of the inflection point and T_N that corresponding to 50 mK. Specific-heat measurements provide a more accurate means of determining $T_N(H)$; see Refs. 28 and 33.

[28] J. S. Kim, J. Alwood, G. R. Stewart, J. L. Sarrao, and J. D. Thompson, Phys. Rev. B **64**, 134524 (2001).

[29] T. Takeuchi, T. Inoue, K. Sugiyama, D. Aoki, Y. Tokiwa, Y. Haga, K. Kindo, and Y. Onuki, J. Phys. Soc. Jpn. **70**, 877 (2001).

[30] D. Hall, E. C. Palm, T. P. Murphy, S. W. Tozer, C. Petrovic, E. Miller-Ricci, L. Peabody, C. Q. Huei-Li, U. Alver, R. G. Goodrich, J. L. Sarrao, P. G. Pagliuso, J. M. Wills, and Z. Fisk, Phys. Rev. B **64**, 064506 (2001).

[31] M. F. Hundley, P. G. Pagliuso, J. L. Sarrao, T. A. Brandman, J. M. Wills, and J. D. Thompson (unpublished).

[32] A similar conclusion has been reached from dHvA measurements. See U. Alver, R. G. Goodrich, N. Harrison, D. W. Hall, E. C. Palm, T. P. Murphy, S. W. Tozer, P. G. Pagliuso, N. O. Moreno, J. L. Sarrao, and Z. Fisk, Phys. Rev. B **64**, 180402(R) (2001).

[33] A. L. Cornelius, P. G. Pagliuso, M. F. Hundley, and J. L. Sarrao, Phys. Rev. B **64**, 144411 (2001).
[34] Wei Bao (private communication).
[35] P. G. Pagliuso, N. J. Curro, N. O. Moreno, M. F. Hundley, J. D. Thompson, J. L. Sarrao, and Z. Fisk (unpublished).
[36] A. D. Christianson, J. M. Lawrence, P. G. Pagliuso, N. O. Moreno, J. L. Sarrao, J. D. Thompson, P. S. Riseborough, S. Kern, E. A. Goremychkin, and A. H. Lacerda (unpublished).
[37] F. Lapierre and P. Haen, J. Magn. Magn. Mater. **108**, 167 (1992).
[38] T. Fukuhara, K. Maezawa, H. Ohkuni, J. Sakurai, and H. Sato, J. Magn. Magn. Mater. **140–144**, 889 (1995).
[39] A. de Visser, J. J. M. Franse, and A. Menovsky, J. Magn. Magn. Mater. **43**, 43 (1984).
[40] A. Amato, D. Jaccard, E. Walker, and J. Flouquet, Solid State Commun. **55**, 1131 (1985).
[41] A. K. Bhattacharjee, B. Coqblin, M. Raki, L. Forro, C. Ayache, and D. Schmitt, J. Phys. (France) **50**, 2781 (1989).
[42] R. A. Steeman, E. Frikkee, R. B. Helmholdt, A. A. Menovsky, J. van den Berg, G. J. Nieuwenhuys, and J. A. Mydosh, Solid State Commun. **66**, 103 (1988).
[43] W. Assmus, M. Herrmann, U. Rauchschwalbe, S. Rigel, W. Lieke, H. Spille, S. Horn, G. Weber, F. Steglich, and G. Cordier, Phys. Rev. Lett. **52**, 469 (1984).
[44] S. Kashiba, S. Maekawa, S. Takahashi, and M. Tachiki, J. Phys. Soc. Jpn. **55**, 1241 (1986); N. Kawakami, A. Nakamura, and A. Okiji, *ibid.* **57**, 4359 (1988).
[45] S. M. M. Evans, A. K. Bhattacharjee, and B. Coqblin, Physica B **165&166**, 413 (1990); Phys. Rev. B **45**, 7244 (1992).
[46] B. Coqblin, A. K. Bhattacharjee, and S. M. M. Evans, J. Magn. Magn. Mater. **90&91**, 393 (1990); M. Raki, L. Forro, C. Ayache, D. Schmitt, A. K. Bhattacharjee, and B. Coqblin, Physica B **163**, 93 (1990).
[47] U. Rauchschwalbe, Physica B **147**, 1 (1987).
[48] G. M. Roesler, Jr. and P. M. Tedrow, Phys. Rev. B **45**, 12 893 (1992).
[49] J. Flouquet, P. Haen, F. Lapierre, D. Jaccard, and G. Remenyi, J. Magn. Magn. Mater. **54–57**, 322 (1986).
[50] M. C. Aronson, J. D. Thompson, J. L. Smith, Z. Fisk, and M. W. McElfresh, Phys. Rev. Lett. **63**, 2311 (1989).
[51] U. Rauchschwalbe, F. Steglich, and H. Rietschel, Physica B **148B**, 33 (1987).
[52] F. B. Anders and M. Huth, Eur. Phys. J. B **19**, 491 (2001).
[53] M. D. Daybell and W. A. Steyert, Phys. Rev. Lett. **18**, 398 (1967); **20**, 195 (1968); E. T. Hedgcock, W. B. Muir, T. W. Raudorf, and R. Szmidt, *ibid.* **20**, 457 (1968); H. Rohrer, Phys. Rev. **174**, 583 (1968).
[54] P. Monod, Phys. Rev. Lett. **19**, 1113 (1967); R. More and H. Suhl, *ibid.* **20**, 500 (1968); M.-T. Béal-Monod and R. A. Weiner, Phys. Rev. **170**, 552 (1968).